Table 1 Maximum error of the approximations

Equation	Z1	Z2	Maximum error	Péclet number
(2)	2.0	——	0.313	2.0
(13)	——	——	0.236	12.9
(15a)	10.0	11,013	0.00045	10.0
(15a)	12.61	150,000	0.000042	12.61
(15b)	10.0	2 × 68	0.00045	10.0

the finite approximations based on Eqs. (15a) and (15b) performed best. In terms of speed it was found that no significant change resulted from employing a 150,000 element array as indicated in Table 1. In the context of the times shown in Fig. 1, the overhead to generate such an array was less than 3 s.

V. Conclusion

The derivation of the exponential-free modified hybrid approximation was motivated by the need to deal as efficiently as possible with the weighting functions arising in the physically based interpolation scheme considered. The alternative approximations, however, clearly appear to represent the most efficient option examined and, in general, can be very effective whenever a parametric dependence on a few variables arises in lengthy calculations. Their accuracies are fully adjustable at the cost of memory allocated rather than computational speed.

References

[1]Spalding, D. B., "A Novel Finite Difference Formulation for Differential Expressions Involving both First and Second Derivatives," *International Journal for Numerical Methods in Engineering*, Vol. 4, No. 4, 1972, pp. 551–559.

[2]Pulliam, T.H., "Artificial Dissipation Models for the Euler Equations," *AIAA Journal*, Vol. 24, No. 12, 1986, pp. 1931–1940.

[3]Peric′, M., "Analysis of Pressure-Velocity Coupling on Nonorthogonal Grids," *Numerical Heat Transfer*, Pt. B, Vol. 17, No. 1, 1990, pp. 63–82.

[4]Leonard, B. P., and Mokhtari, S., "Beyond First-Order Upwinding: The ULTRA-SHARP Alternative for Non-Oscillatory Steady-State Simulation of Convection," *International Journal for Numerical Methods in Engineering*, Vol. 30, No. 4, 1990, pp. 729–766.

[5]Shyy, W., Thakur, S., and Wright, J., "Second-Order Upwind and Central Difference Schemes for Recirculating Flow Computation," *AIAA Journal*, Vol. 30, No. 4, 1992, pp. 923–932.

[6]Raithby, G. D., "Skew Upstream Differencing Schemes for Problems Involving Fluid Flow," *Computer Methods in Applied Mechanics and Engineering*, Vol. 9, 1976, pp. 153–164.

[7]Baliga, B. R., and Patankar, S.V., "A Control Volume Finite-Element Method for Two-Dimensional Fluid Flow and Heat Transfer," *Numerical Heat Transfer*, Vol. 6, No. 3, 1983, pp. 245–261.

[8]Prakash, C., "An Improved Control Volume Finite-Element Method for Heat and Mass Transfer, and for Fluid Flow Using Equal-Order Velocity Pressure Interpolation," *Numerical Heat Transfer*, Vol. 9, No. 3, 1986, pp. 253–276.

[9]Schneider, G. E., and Raw, M. J., "Control Volume Finite-Element Method for Heat Transfer and Fluid Flow Using Colocated Variables - 1. Computational Procedure," *Numerical Heat Transfer*, Vol. 11, No. 4, 1987, pp. 363–390.

[10]Thiart, G. D., "Improved Finite-Difference Scheme for the Solution of Convection-Diffusion Problems with the SIMPLEN Algorithm," *Numerical Heat Transfer*, Pt. B, Vol. 18, No. 1, 1990, pp. 81–95.

[11]Rhie, C. M., and Chow, W. L., "Numerical Study of Turbulent Flow Past an Airfoil with Trailing Edge Separation," *AIAA Journal*, Vol. 21, No. 11, 1983, pp. 1525–1532.

[12]Harms, T. M., von Backström, T. W., and Du Plessis, J. P., "Reformulation of the SIMPLEN Discretization Scheme to Accommodate Noncentralized Interfaces," *Numerical Heat Transfer*, Pt. B, Vol. 20, No. 2, 1991, pp. 127–144.

[13]Huang, P. G., Launder, B. E., and Leschziner, M. A., "Discretization of Nonlinear Convection Processes: A Broad-Range Comparison of Four Schemes," *Computer Methods in Applied Mechanics and Engineering*, Vol. 48, No. 1, 1985, pp. 1–24.

[14]Karki, K. C., Patankar, S. V., and Mongia, H. C., "Three-Dimensional Fluid Flow Calculations Using a Flux-Spline Method," *AIAA Journal*, Vol. 28, No. 4, 1990, pp. 631–634.

[15]Harms, T. M., Du Plessis, J. P., and von Backström, T. W., "Derivation of a Modified Power-Law Approximation," *Numerical Heat Transfer*, Pt. B, Vol. 22, No. 2, 1992, pp. 235–241.

Approximations for Weak and Strong Oblique Shock Wave Angles

Anthony M. Agnone*
Hofstra University, Hempstead, New York 11550

Introduction

IN fluid mechanics computations, such as in the study of shock-boundary layer interactions, the oblique shock wave angle is needed as an explicit function of the upstream Mach number M and the flow turning angle δ. In Ref. 1, approximate shock-flow angle relations are developed from series expansions of the exact equation [Eq. (1) of Ref. 1]. The resulting expressions [Eqs. (13) and (14) of Ref. 1] are limited to weak oblique shocks and small wedge angles. In Ref. 2, it is commented that those approximate relations do not asymptote correctly in the limit of the infinite Mach number. Here, a simple exact explicit relation is obtained for the case of an infinite Mach number that is valid for both weak and strong shocks. Approximate relations for both weak and strong shocks are also derived for finite Mach numbers and moderate wedge angles.

Derivation of Equations

Equation 1 of Ref. 1, [or Eq. (148) of Ref. 3] can be recast into a cubic equation for the square of the sine of the shock wave angle θ as follows [see Eq. (150a) of Ref. 3]:

$$\sin^6\theta + b\sin^4\theta + c\sin^2\theta + d = 0 \tag{1a}$$

where

$$b = -(M^2 + 2)/M^2 - \gamma\sin^2\delta \tag{1b}$$

$$c = (2M^2 + 1)/M^4 + [(1/4)(\gamma + 1)^2 + (\gamma - 1)/M^2]\sin^2\delta \tag{1c}$$

$$d = -\cos^2\delta/M^4 \tag{1d}$$

and γ is the ratio of specific heats. Exact explicit equations for the three real roots of this cubic equation can be found in Ref. 4; however they are not easily approximated. Here simple relations are derived by noting that in the limit of infinite Mach number, the coefficient d vanishes and b and c simplify to

$$b' = -1 - \gamma\sin^2\delta \tag{2a}$$

and

$$c' = [(\gamma + 1)^2/4]\sin^2\delta \tag{2b}$$

Then Eq. (1a) is reduced to a quadratic and its two roots can be obtained from

$$\sin^2\theta_\infty = (1/2)[-b' \pm (b'^2 - 4c')^{1/2}] \qquad \text{for } M_\infty \to \infty \tag{3}$$

The positive and negative signs correspond to the strong and weak shock, respectively. This equation is represented graphically in Fig. 1 for $\gamma = 1.4$ and is compared with $\theta \approx (\gamma + 1)\,\delta/2$, [Eq. (3a) of Ref. 5]. As shown in Fig. 1, the latter is accurate for $\delta < 25$ deg. The disappearance of the third but physically inadmissible root is evident from the shock polar in that the limit circle (for $M = \infty$) coincides with the approach flow circle.

Approximate but accurate relations for finite Mach numbers are obtained by noting that d is small since it depends inversely on the

Received Oct. 4, 1993; revision received Feb. 23, 1994; accepted for publication March 5, 1994.

*Associate Professor, Department of Engineering. Senior Member AIAA.

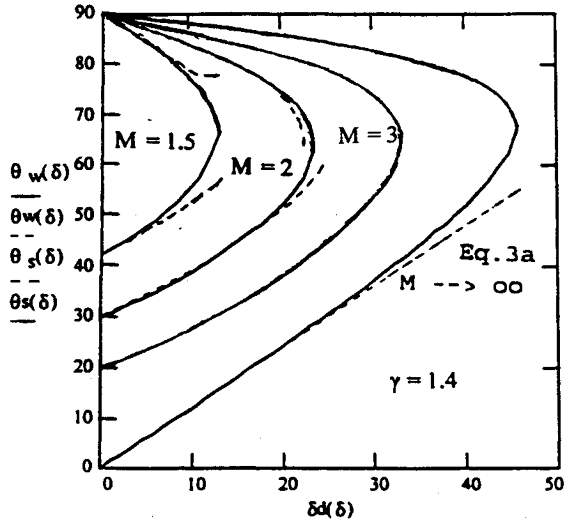

Fig. 1 Comparison of exact and approximate solutions for several Mach numbers.

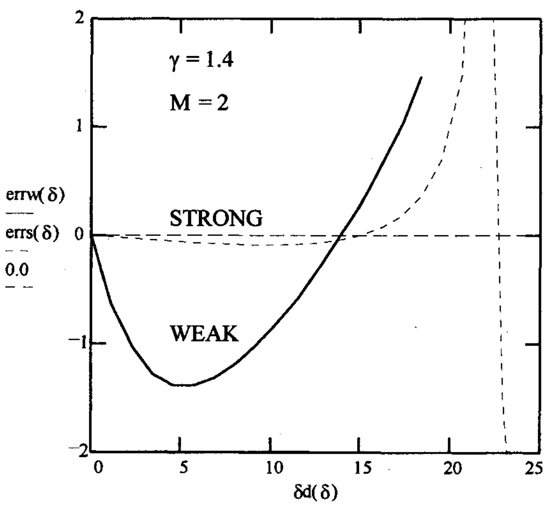

Fig. 2 Error incurred using present approximation for M = 2.

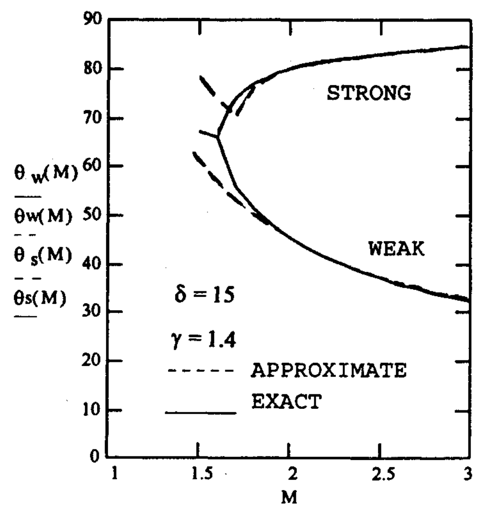

Fig. 3 Comparison of exact and approximate solutions for δ = 15 deg.

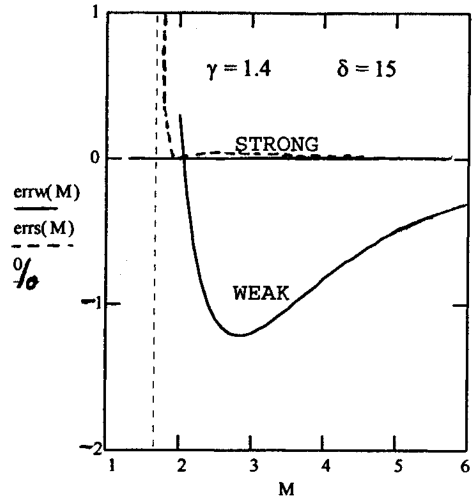

Fig. 4 Error incurred using present approximation for δ = 15 deg.

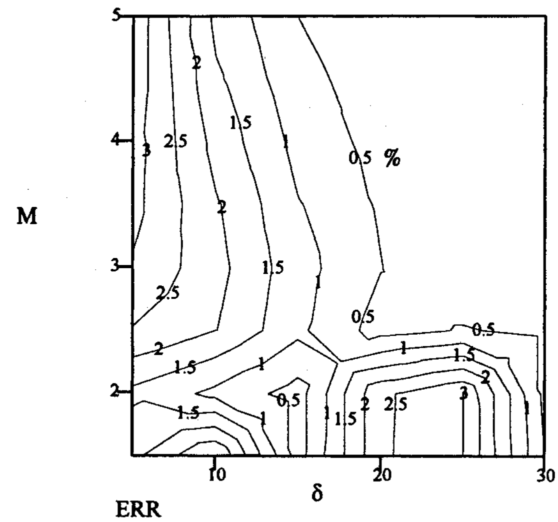

Fig. 5 Relative percent error isolines of the present approximation for the weak shock angle.

fourth power of the Mach number. Then the cubic equation is approximated by a quadratic by dividing through by $\sin^2\theta$, to obtain

$$\sin^4\theta + b\sin^2\theta + (c + d/\sin^2\theta_{w\text{ or }s}) \approx 0 \tag{4}$$

Then using the Mach angle

$$\mu = \sin^{-1}(1/M) \tag{5}$$

set

$$\theta = \theta_w \approx \delta + \mu \tag{6}$$

and

$$\sin^2\theta = \sin^2\theta_s \approx 1 - [\gamma - (1/4 - \gamma/M^4)(\gamma + 1)^2]\sin^2\delta \tag{7}$$

for weak and strong shock angles, respectively in the $\sin^2\theta$ term, which divides the coefficient d. Then solve Eq. (4) to get

$$\sin^2\theta \approx (1/2)\left[-b \pm [b^2 - 4(c - d/\sin^2\theta_{w\text{ or }s})]^{1/2}\right] \tag{8}$$

The ± signs have the same meaning as previously.

Results

A comparison of Eq. (8) with the exact solution is also shown in Fig. 1 for several approach Mach numbers. As shown in Fig. 2, for M = 2 the error is less than 2% and is largest near the maximum deflection angle δ_{max}. A comparison of the present and exact solutions is shown in Fig. 3 as a function of Mach number for both weak and strong shocks and for δ = 15 deg. As shown in Fig. 4, the error decreases rapidly at high Mach numbers. Whereas, as shown in Fig. 3 of Ref. 1, the error incurred using their approximations increases as the Mach number or wedge angle increases. The relative percent error isolines of the present approximation are shown in

Fig. 5 for the weak shock solution. The relative error of the strong shock approximation are even smaller.

Conclusion

Approximate relations for both weak and strong oblique shock angles have been shown to be accurate for moderate to high supersonic Mach numbers and for wedge angles that are less than the maximum wedge angle.

References

[1]Dou, H. S., and Teng, H.-Y., "Approximate Formula of Weak Oblique Shock Wave Angle," *AIAA Journal,* Vol. 30, No. 3, 1992, pp. 837–839.

[2]Powers, J. M., "Comment on 'Approximate Formula of Weak Oblique Shock Wave Angle,'" *AIAA Journal,* Vol. 30, No. 11, 1992, pp. 2801, 2802.

[3]Anon., "Equations, Tables and Charts for Compressible Flow," Ames Aeronautical Lab., TR 1135, Moffett Field, CA, 1953

[4]Mascitti, V. R., "A Closed-form Solution to Oblique Shock-Wave Properties," *Journal of Aircraft,* Vol. 6, No. 1, 1969, p. 66.

[5]Liepman, H. W., and Roshko, A., *Elements of Gas Dynamics,* Wiley, New York, 1957, pp. 84–93.

Adaptive Computations of Flow Around a Delta Wing with Vortex Breakdown

David L. Modiano* and Earll M. Murman†
Massachusetts Institute of Technology, Cambridge, Massachusetts 02139

I. Introduction

THE next generation of fighter aircraft is being designed to fly at very high angle of attack, at which vortex breakdown occurs.[1] The two typical types of breakdown are the "bubble" form and the "spiral" form, which are characterized by the geometry of the flow downstream of the breakdown. This Note presents simulations of vortex breakdown above a stationary delta wing over a range of angles of attack. Adaptive refinement is used to add mesh nodes in the region of the vortex. Numerical simulations of vortex breakdown over a stationary delta wing have been reported by various researchers. No calculations have been reported using adaptive mesh methods.

II. Solution Method

Full details can be found in Ref. 2. The governing equations are the Euler equations for inviscid, compressible flow. The spatial discretization is a node-based trilinear Galerkin finite element method. Tetrahedral cell meshes are generated by the advancing wave front method of Peraire et al.[3] A mix of second- and fourth-difference artificial dissipation is added to insure stability. The fourth difference is constructed so that it vanishes when applied to a linear function, using the method of Holmes and Connell.[4] Temporal integration is performed by the four-stage method of Jameson et al.,[5] based on the Runge-Kutta method. The artificial dissipation is frozen after the second stage. Local time steps are used for steady flow solutions, based on an energy stability analysis by Giles.[6]

III. Adaptation Procedure

Adaptive mesh-point embedding is used to increase the mesh resolution in the vicinity of interesting flow features. The adaptation procedure is as follows. The adaptation parameter is calculated at the mesh nodes. The nodes are marked for adaptation where the adaptation parameter exceeds a threshold. A mesh cell is subdivided into 12, 4, or 2 smaller cells, depending on how many of its corners are marked.

The entropy and the total pressure loss are attractive adaptation parameters for vortex flows, since they vanish in the irrotational limit. Both have been used successfully as adaptation parameters for delta wing flows.[7,8] In the present work the entropy was chosen, with the adaptation threshold set so that 30% of the coarse mesh nodes would be marked for refinement. This fraction was chosen so that the entire vortex is included in the adapted region, and it results in a quadrupling of the number of nodes and cells of the mesh.

IV. Stationary Wing Solutions

Stationary wing solutions were obtained at eight values of angle of attack, in the range of 0 to 42 deg. The angles of attack are concentrated in the high part of the range, in which vortex breakdown occurs. The leading-edge sweep back angle Λ is 75 deg, so the aspect ratio is 1.07. The freestream Mach number $M_\infty = 0.3$ for all cases. The geometry and Mach number were chosen to match those used by Ekaterinaris and Schiff[9] for their solutions.

The coarse mesh used for all cases has 15,462 nodes. The adapted meshes vary from 77,630 to 83,286 nodes.

A. Analysis of Global Features of Solutions

Stationary wing normal force curves are presented in Fig. 1, compared with Jarrah's wind tunnel-data.[10] Where two symbols are shown for the same angle of attack, the solution does not converge, which for the cases involving vortex breakdown is due to the inherent unsteadiness of the flow downstream of breakdown. The normal force coefficient is adequately predicted using the coarse mesh at low angles of attack, in which the vortex is intact over the entire wing. However, the coarse mesh is insufficient to

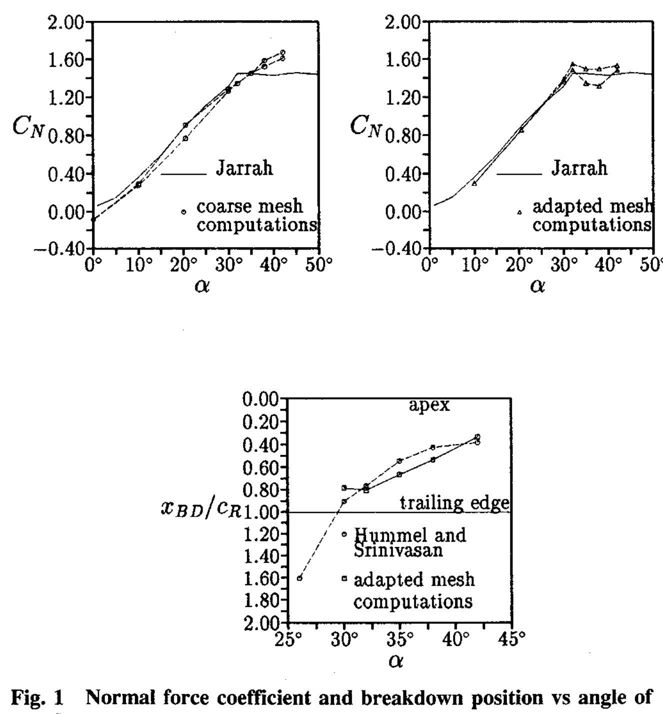

Fig. 1 Normal force coefficient and breakdown position vs angle of attack.

Received May 4, 1993; presented as Paper 93-3400 at the AIAA 11th Applied Aerodynamics Conference, Monterey, CA, Aug. 9–11, 1993; revision received Oct. 21, 1993; accepted for publication Oct. 21, 1993.

*Research Assistant, Computational Aerospace Sciences Laboratory, Deptartment of Aeronautics and Astronautics; currently Senior Research Associate, ICOMP, NASA Lewis Research Center, Cleveland, OH 44135. Member AIAA.

†Professor and Head, Deptartment of Aeronautics and Astronautics. Fellow AIAA.